Automatic detection of number of aircrafts over satellite data using deep learning

Jai Gopal Singla*

Space Application Centre, ISRO, Ahmedabad
Gujarat, India
Email: jaisingla@sac.isro.gov.in

Gautam Kumar Jaiswal

HMR Institute of Technology and Management
Delhi, India
Email: gautamjaiswal030@gmail.com

Renu Chaudhary

HMR Institute of Technology and Management
Delhi, India
Email: mail.renuchaudhary@gmail.com

Darshan Kumar Patel

Space Application Centre, ISRO, Ahmedabad
Gujarat, India
Email: dk@sac.isro.gov.in

This paper in non peer-reviewed preprint submitted to EarthArXiv.

Abstract: Instance segmentation is a novel technique to automatically detect and count the number of objects from satellite imagery for various applications using deep learning frameworks such as Mask-RCNN and YOLO. In this paper, we have implemented the YOLOv5 and YOLOv7 instance segmentation models on high-resolution satellite imagery (0.31m to 1.74m) of both panchromatic (16-bit PAN) and multi-Spectral (16-bit 9-channels MS) sensors and evaluated the comparative performance of these models. After training both the models on 300 epochs, the models showed very good comparative accuracies. YOLOv7 outperformed YOLOv5 on Mean Average Precision (mAP) parameter with of 99.20% mAP value as compared to YOLOv5's 99.12% mAP value. We have also obtained the model results on panchromatic and multi-spectral remote sensing data of Indian remote sensing data over Mumbai, Pune, and Ahmedabad airports with an accuracy of above 94% to segment the larger aircrafts and above 88% to segment smaller aircrafts

Keywords: Instance Segmentation, Aircraft Detection, YOLO v7, YOLO v5, Satellite Imagery, Remote sensing

1 Introduction

Remote sensing and very high-resolution imagery data from satellites help to detect objects from the space and provides the required input data to monitor the object's position and shape accurately using instance segmentation. Our study mainly focused on instance segmentation models for detection and counting the number of aircraft and to evaluate the latest-best "State-of-The-Art" deep learning algorithms for this cause.

Several researchers across the Globe has worked towards this challenging problem. Abhimanyu Singh et al (2022) implemented the YOLOv7 object detection framework on Airbus Aircraft Detection Dataset to identify the aircraft in satellite images with the max mAP and F1 score of 0.84 and 0.81 on SGD optimizer [1]. Shenglong Chen et al (2022) proposed a framework solution for scene classification, building instance segmentation and color normalization on low-resolution satellite imagery using Improvised Mask R-CNN with MPViT backbone achieved the F1 scores of 0.71, 0.70, 0.81, and 0.67 for non-built-up, rural, suburban, and urban areas [2]. T. Wang et al (2021) worked on a high-resolution remote sensing satellite dataset of landslides and improvement in the backbone architecture of the YOLOv5 model. They introduced the Adaptively Spatial Feature Fusion (ASFF), feature fusion-slicing method to improve feature information on different scales for better model accuracy by 0.52% and Convolutional Block Attention Module (CBAM) to the backbone to restore the spatial information, and improved the performance by 1.12% [3]. Shunjun Wei et al (2020) constructed the High-Resolution SAR Image Dataset (HRSID) for ship detection and instance segmentation. In this paper, they have implemented the Mask R-CNN and Cascade Mask R-CNN with the backbone of ResNet50-FPN and ResNet101-FPN with the validated overall performance in terms of Average Precision (AP) above 86% [4]. Ismail Karakaya et al (2020) worked on satellite images objects classification and implemented the ensemble model of Faster R-CNN with U-Net for objects segmentation (ships, vessels, oil tanks, heliport, airplane, and buildings) in satellite images [5]. Merve Polat et al (2019) implemented the CNN-based algorithm AlexNet to train the initial model and further used Faster R-CNN using transfer learning technique to improve the average precision of the model to 91% [6]. Lichao Mou et al (2018) proposed a novel semantic boundary-aware unified multitask learning ResFCN (Residual Fully Connected Network) for instance segmentation of vehicles in aerial images using both ISPRS Potsdam Semantic Labeling and Busy Parking Lot UAV Video data set. The highest model performance of ResFCN improved by F1 equal to 0.98 frame per second with a precision of 1.0 [7]. Hui Wu et al (2015) proposed a framework for fast aircraft detection in satellite images using the BING technique and CNN trained on a custom satellite dataset of aircraft from Google Earth. This experiment has shown the detection on different

scales with the highest performance of Precision-Recall by 92% [8].

We initiated our work on instance segmentation using high-resolution data of both panchromatic (PAN) and multi-spectral (MS) captured using Maxar Worldview-3 mission, SPOT, and Vision-1 satellites (0.3m to 1.21m spatial resolution). The YOLOv5 and YOLOv7 models were trained to obtain instance segmentation results and count the aircraft. Using the proposed models, a testing accuracy of 0.993 is achieved at the 0.5 IoU threshold on unseen data. Further, 0.94 accuracies (under 0.25 confidence threshold) were achieved on panchromatic and multi-spectral remote sensing data captured using Indian remote sensing data over Mumbai, Pune, and Ahmedabad airports. This work highlights the importance of high-resolution satellite imagery to detect and automatically count the number of objects using deep learning.

2 Background Study

(a) Object Detection with Deep Learning

Object detection using deep neural networks are used to identify and localize objects within an image or video. Object detection is a fundamental task in computer vision and has a wide range of applications, such as self-driving cars, surveillance systems, and image search. The most popular deep learning architecture for object detection is the Convolutional Neural Network (CNN) [9]. CNNs are powerful because they can learn features that are relevant to object detection directly from the data. There are many CNN-based object detection frameworks available, such as YOLO (You Only Look Once), Faster R-CNN (Region-based Convolutional Neural Network), and SSD (Single Shot Detector) [10].

(b) Deep Learning on Satellite Data

Deep learning on satellite data is used to perform a wide range of tasks, such as land cover classification, small object detection, image segmentation, and change detection. Satellite data provides a unique perspective on the Earth's surface and can be used to monitor environmental changes, track urbanization, and support disaster response efforts. The main challenge in applying deep learning in satellite data is the large size and high data dimensions. Satellite images typically have high spatial resolution and cover a large area, which can result in millions or billions of pixels per image. Moreover, satellite images often have multiple bands, such as red, green, blue, and infrared, which further increases the dimensions of the data. To overcome these challenges, researchers have developed a variety of deep learning architectures and techniques that are specifically designed for satellite data. For example, Convolutional Neural Networks (CNNs) can be used to automatically learn features from satellite images that are relevant for a particular task, such as instance segmentation of aircraft and land cover classification. Recurrent Neural Networks (RNNs) can be used to process time series data from satellites, such as the Normalized Difference Vegetation Index (NDVI) and Change detection over multiple years. Another popular technique for deep learning with satellite data is Transfer Learning. Transfer learning involves pre-training a deep learning model on a large dataset, such as ImageNet, and then fine-tuning the model on a smaller dataset of satellite images. This approach can significantly reduce the amount of labeled data required for training, while also improving the generalized performance of the model [11].

(c) Instance Segmentation

Instance segmentation is a computer vision task that involves identifying and segmenting individual objects within an image or video. Unlike semantic segmentation, which groups pixels into regions based on their semantic meaning (e.g., car, cloud, person, aircraft), instance segmentation differentiates between individual objects of the same class (e.g., two aircraft or

two people) and assigns them separate labels [12]. There are two most commonly used methods Mask R-CNN, which builds on the popular Faster R-CNN architecture by adding a mask branch that generates a binary mask for each detected object. The mask branch uses a Fully Convolutional Network (FCN) to predict a binary mask for each object instance, which can then be used to segment the object from the background [13]. Second, BlendMask is an instance segmentation framework built on top of the FCOS object detector. The bottom module uses either backbone or FPN features to predict a set of bases. A single convolution layer is added on top of the detection towers to produce attention masks along with each bounding box prediction. For each predicted instance, the blender crops the bases with its bounding box and linearly combines them according to the learned attention maps [14].

(d) Evolution of YOLO

YOLO (You Only Look Once) is a widely used object detection algorithm designed by Redmon et al [15] in 2015. YOLO algorithm is based on Convolutional Neural Networks (CNN) that has 24 convolutional layers, 4 max pooling layers and 2 fully connected layers. It is a single-shot object detection algorithm runs an input image and computes the results through localizing the object with predicted class at once. Popular object recognition framework YOLO has experienced multiple revisions, each with its own improvements and benefits. The initial version of YOLO, known as v1, was released in 2015. A real-time object detection system predicted object classes and bounding boxes from a whole image using a single Convolutional Neural Network (CNN). Although YOLO v1 was quick, it had poorer detection precision for small and overlapping objects. The accuracy difficulties with YOLO v1 were addressed in YOLO v2, which was released in 2016. To increase detection precision for small objects and decrease false positives, it implemented a number of innovations, including batch normalization, anchor boxes, and multi-scale training. On the PASCAL VOC and COCO datasets, YOLO v2 demonstrated cutting-edge performance. With a number of new features, including Feature Pyramid Networks (FPN), enhanced anchor box clustering, and a new backbone architecture based on DarkNet-53, YOLO v3 was introduced in 2018 and substantially enhanced YOLO v2. Compared to YOLO v2, v3 achieves even greater accuracy and faster performance. A framework called YOLOACT combines YOLOv3 for object detection with ACT (Action Constrained Temporal Convolutional) neural networks for action recognition. With the help of the YOLOACT framework, it is possible to jointly identify objects and actions in films, which is helpful for a number of applications like surveillance, sports analysis, and human-computer interaction. The YOLOv3 detector is used to find and track the objects involved in those actions, while the ACT neural network is used to identify human actions from a temporal sequence of frames. A number of additional features, including the scaled-YOLOv4 architecture, the MISH activation function, the Spatial Pyramid Pooling (SPP), the Path Aggregation Network (PAN), and the Cross Stage Partial Network (CSP), were included in the introduction of YOLO v4 in 2020. On the COCO dataset, YOLO v4 outperformed other object identification frameworks like EfficientDet and DETR [16], achieving state-of-the-art performance.

3 Dataset Details

We have taken CosmiQ Works RarePlanes and Airbus High-Resolution Satellite Imagery datasets to implement aircraft detection in satellite data. CosmiQ Works and AI.Reverie developed an open-source machine learning dataset name RarePlanes that incorporates both real and synthetic-generated satellite imagery. We have taken 253 Maxar WorldView-3 satellite real data that spans from 113 locations in 22 countries over the world which covers around 2,142 km^2 areas at the off-nadir (satellite angle concerning its target at the time of collection) 3.2 to 29.6 degrees comprises of 8-bit RGB, 16-bit 9-channels Multi-Spectral (MS) and 16-bit Panchromatic (PAN) very high-resolution satellite imagery at the 0.3 to 1.25 spatial resolution [17]. The Second Airbus Aircraft Detection dataset consists of optical satellite imagery from SPOT, Vision-1, and Pleiades commercial satellites from various airport

locations at roughly 0.5 resolution [18].

Sr. no	Product ID	Date of Pass	Orbit No	Satellite id	Sensors	Site	Resolution
1.	16229811	31MAR2017	669	Cartosat-2S	PAN	Pune	0.65m
2.	16295241	18-Feb-2017	47		PAN and MX	Mumbai	0.65-1.6m
3.	16769611	24-Feb-2017	138		MX	Ahmedabad	1.6m

Table 1. Dataset details of Indian Remote Sensing mission.

4 Methodology

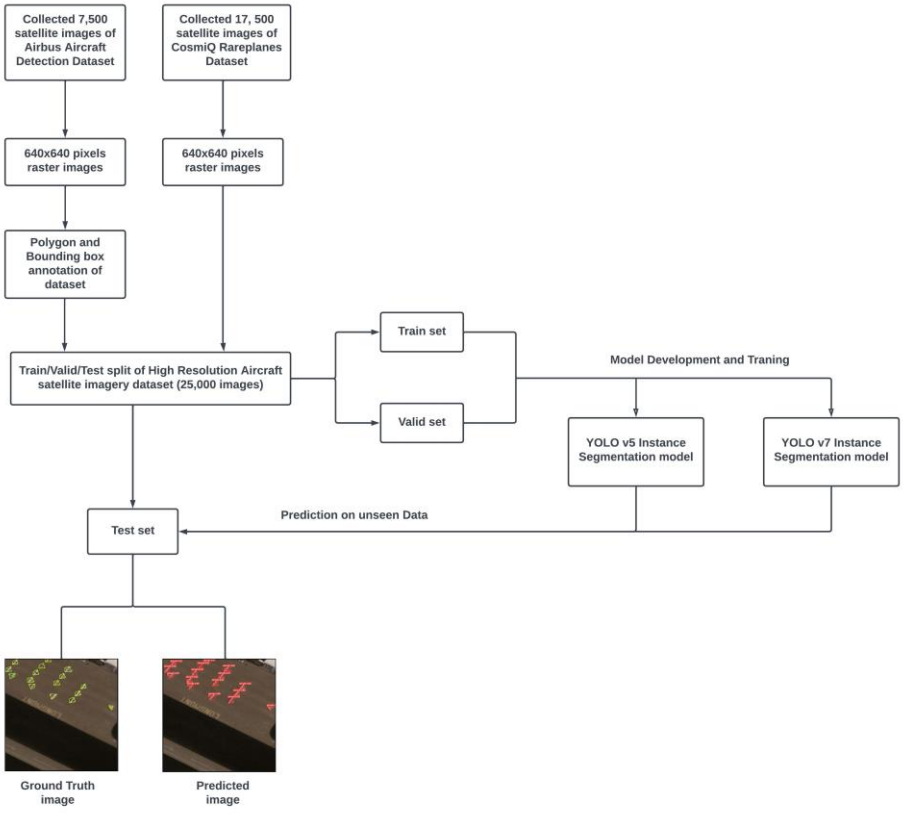

Fig. 1. The Process Flow Diagram

(a) Preparation and Processing of Dataset

RarePlanes and Airbus Aircraft Detection datasets provide a large number of Very High-Resolution Satellite data over many locations of airports. For the study, we built the dataset of 25,000 images of both RarePlanes and Airbus data in the ratio of 7:3 (17500 images of the RarePlanes of both Multi-Spectral and Panchromatic (PAN) and 7500 images of the Airbus Aircraft Detection). During the Pre-Processing of the dataset, we resize the dataset into 640x640 pixels raster images. We have used LabelMe offline annotation tool, for instance, segmentation that supports the polygon shape labeling feature to annotate the 7500 images of the Airbus Aircraft dataset in the shape of a pyramid as per the RarePlanes annotation guidelines. After that, we split the data into a training set (21,000 images) and a validation set (3000 images) to train the models and 1000 images to test the models on unseen images.

5 Model Architecture

(a) YOLO v5

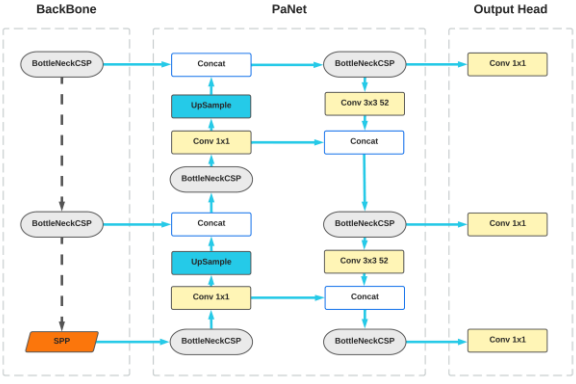

Fig. 2. The Architecture of YOLOv5.

YOLOv5 is a popular object detection algorithm in the You Only Look Once (YOLO) family. YOLOv5 generally uses a combination of different architectures to improve its performance. The backbone architecture used in YOLOv5 is CSPDarknet53, a variant of the DarkNet architecture. It uses Cross-Stage Partial Connections (CSP) to improve the representation power of the model. The SPP layer [19] is added to the CSPDarknet53 to improve the model's ability to handle objects of different scales. The Neck architecture used in YOLOv5 is PANet (Path Aggregation Network) [20] which helps to improve the feature pyramid and multi-scale context aggregation. The YOLO detection head is a Convolutional Neural Network (CNN) architecture used to predict the bounding boxes and class probabilities of objects in an image.

To further optimize the whole architecture, YOLO v5 provides a set of techniques called a "bag of freebies and specials". Bag-of-freebies are modifications to the architecture that improve the performance of the model without adding additional computational costs. "Specials" are techniques that are added to the architecture to improve the performance of the model, but they may increase the computational cost [21].

(b) YOLO v7

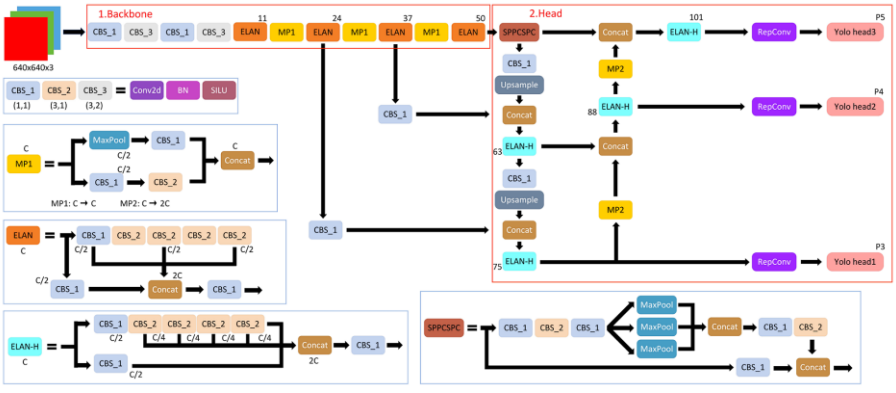

Fig. 3. The Architecture of YOLOv7 [22].

Wang, C.Y. et al (2022) introduced YOLOv7 which is an improved version of YOLOv5 in image segmentation, especially focused on instance segmentation. They surpassed all previous real-time object detection and instance segmentation algorithms in both speed and accuracy with 5.6% AP with 30 FPS compared to transformer-based SWINL Cascade-Mask R-CNN, by 509% in speed and 2% in accuracy, and Convolutional based detector ConvNeXt-XL Cascade-Mask R-CNN by 551% in speed and 0.7% AP in accuracy, as well as it outperforms to YOLOR, YOLOX, Scaled-YOLOv4, YOLOv5, DETR, Deformable DETR, DINO-5scale-R50, ViT-Adapter-B and many other object detectors and segmentation in speed and accuracy.

They proposed Extended Efficient Layer Aggregation Networks (E-ELAN) in the backbone that does not change the gradient transmission of the original YOLOv5 architecture that helps with up-sampling and top-down sampling on layers. Other proposed features of YOLOv7 are depth-width-based compound scaling for the concatenation model. Some trainable "Bag-of-Freebies" for improving the training accuracy and performance in which they focused on the re-parameterized convolution of the Res-RepNet model, coarse for auxiliary head loss and fine for lead head loss [23].

6 Evaluation Metrics and Hyperparameters Optimization

During the training of proposed models, to quantify the predicted results and ground truth used intersection over union (IoU), which calculates the difference between each pixel of predicted results and ground truth divided by the total number of pixels contained in both images.

$$IoU = \frac{Predicted\ result \cap Ground\ truth}{Predicted\ result \cup Ground\ truth} \tag{1}$$

We have calculated the mask precision, recall, and mean average precision at an IoU threshold of 0.5 and 0.95 for each image in the training and validation set. Precision shows the percentage of predicted results that were true positives from tested data. Recall shows the percentage of ground truth that is correctly predicted from test data.

$$Precision\ (P) = \frac{True\ Positive}{True\ Positive + False\ Positive} \tag{2}$$

$$Recall\ (R) = \frac{True\ Positive}{True\ Positive + False\ Negative} \tag{3}$$

Mask Mean Average Precision (mAP) calculates the mean of average precision across all classes mask to compare the speed and accuracy of models on the same task (aircraft instance segmentation).

$$Mean\ Average\ Precision\ (mAP) = \frac{1}{n}\sum_{1}^{n} Average\ Precison_k \tag{4}$$

$$n = the\ number\ of\ classes$$
$$k = particular\ class$$

Table 2 enlists some important Hyperparameters and alternate values, which were used during the model's training. The important hyperparameters to train instance segmentation models are soft anchor box, mask ratio, and learning rate, in which soft anchor boxes define the number of auto-generated bounding boxes to detect the instances of objects and mask ratio specifies the segmentation of object region during the training of the model. The learning rate specifies the extent of gradient values toward a minimum of a loss function at each iteration. We have used Stochastic Gradient Descent (SGD) and Adaptive moment estimation (Adam) optimizer with the batch size of 16 and 32 to effectively faster the performance and optimize the weights with the model complexity.

Hyperparameters	Value
Learning rate (lr)	{0.001, 0.01}
Epochs	{50, 100, 300}
Batch size	{16, 32}
Momentum	0.937
Weight decay	{0.0005, 0.001}
Optimizer	{SGD, Adam}
Mask ratio	{0.4, 0.6}
Anchor box	{4, 8}

Table 2. Hyperparameters during training of YOLOv5 and YOLOv7.

7 Results

All the experiments on our dataset are supported by the personal computer (PC) with the x86 64-bit Linux 7.7 (Mapio) operating system. The software configuration consists of Python programming language, PyTorch 1.11, CUDA 12.0, and cuDNN 8.81. The hardware capabilities include NVIDIA Quadro GV100 GPU (64GB memory), Intel Xeon Platinum 8180 CPU @2.50GHz, and 1TB RAM. Comparatively, Both YOLOv5 and YOLOv7 trained on high mosaic hyperparameters along with mentioned hyperparameters in Table 2.

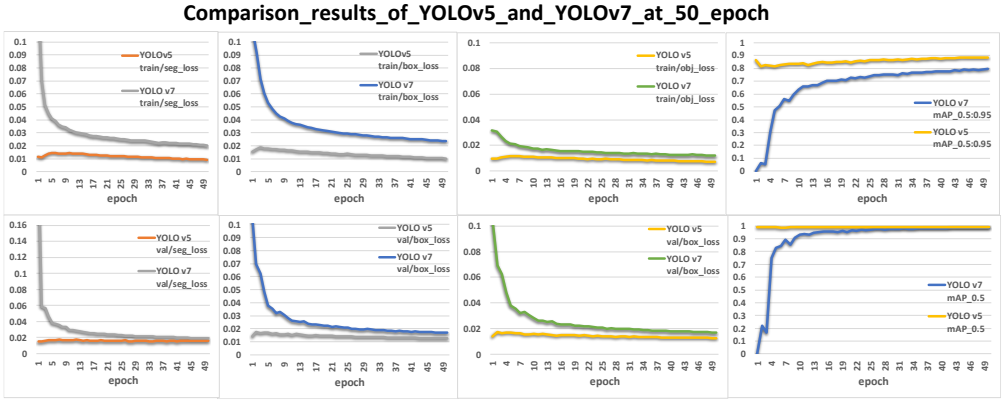

Fig. 4 (a) The comparison graphs of YOLOv5 and YOLOv7 at 50 epochs.

As shown in Fig. 4. (a) Bounding box loss, segmentation loss, and mask mean average precision of YOLOv5 improved by 0.2%, 0.2%, and 0.1% at IoU 0.95 compared to YOLOv7 after training on 50 epochs. As for multi-scale instance segmentation, YOLOv5 was not able to segment small and medium aircraft, and YOLOv7 segments the medium aircraft with good

accuracy above 53%. We continue to train on more iterations to reduce the losses of the models and improve the accuracy. After being trained on 100 epochs, YOLOv7 showed improvement in both segmentation loss and object loss with the mask mAP above 0.832 at 0.95 IoU threshold and mAP of 0.9903 at 0.5 IoU threshold on the other side YOLOv5 shown the decrement in terms of segmentation and bounding box loss by 0.1% as shown in Fig. 4 (b).

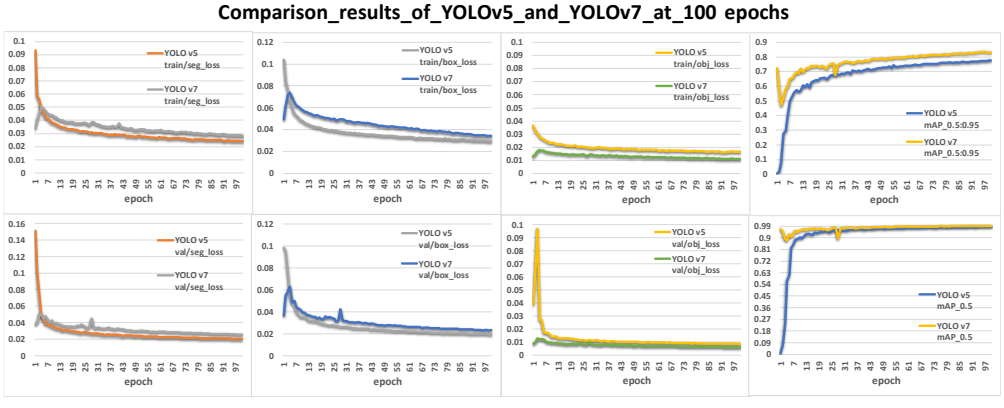

Fig. 4 (b) The comparison graphs of YOLOv5 and YOLOv7 at 100 epochs.

YOLOv7 shows the improvements after getting trained on more iterations of both training and validation data. We increased the IoU and anchor threshold to 0.85 and 0.75 with a 0.01 learning rate to reduce the training and validation losses and improve the mean average precision. We have trained the models on the best 300 epochs, as shown in Fig. 4 (c) YOLOv7 showed an improvement in terms of both training and validation losses and mask mAP by 99.201 % at 0.5 IoU and 85.36% at 0.5:0.95 IoU comparatively YOLOv5 shown the mask mAP of 99.125% and 84.75% at 0.5 and 0.5:0.95 IoU.

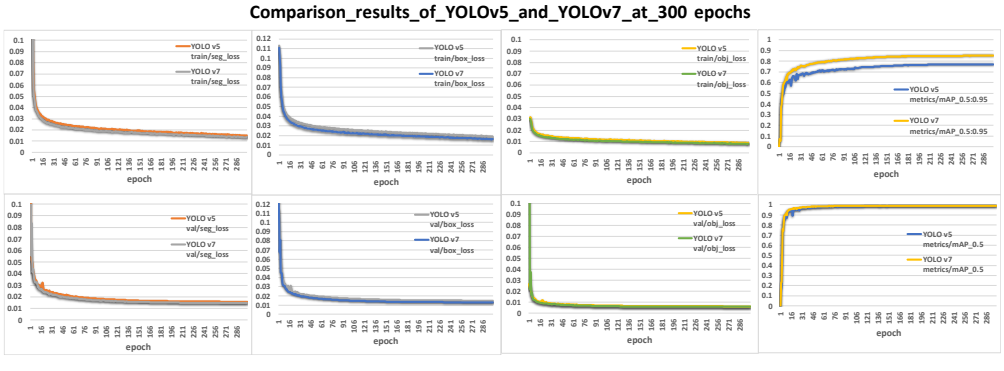

Fig. 4 (c) The comparison graphs of YOLOv5 and YOLOv7 at 300 epochs.

For understanding the models, we have also compared the training and validation segmentation loss, precision, and recall over 50, 100, and 300 epochs as shown in Table 3. Under the bounding box IoU threshold of 0.5, YOLOv7 receives the highest box and mask Precision-Recall score of 0.992 and 0.991 and YOLOv5 receives 0.991 respectively after 300 epochs. YOLOv7 performs better than YOLOv5 in the bounding box and mask mAP with its mask branch and RoI align. Using the stepwise increasing IoU threshold and iterations in each model structure, YOLOv7 receives a prominent improvement of 1.3% and 1.0% than YOLOv5 in mask mAP and segmentation loss.

Model	Epochs	Training Segmentation Loss	Validation Segmentation Loss	Precision	Recall	mAP (Mean Average Precision)
YOLO v5	50	0.009	00153	0.9802	0.970	0.993 (mAP_0.5) 0.886 (mAP_0.5:0.95)
	100	0.024	0.020	0.968	0.951	0.98 (mAP_0.5) 0.77 (mAP_0.5:0.95)
	300	0.014	0.015	0.979	0.976	0.99 (mAP_0.5) 0.84 (mAP_0.5:0.95)
YOLOv7	50	0.020	0.0189	0.978	0.946	0.98 (mAP_0.5) 0.79 (mAP_0.5:0.95)
	100	0.028	0.025	0.979	0.968	0.99 (mAP_0.5) 0.83 (mAP_0.5:0.95)
	300	0.013	0.014	0.986	0.978	0.99 (mAP_0.5) 0.85 (mAP_0.5:0.95)

Table 3. Instance segmentation statistics generated by YOLOv5 and YOLOv7 after 50, 100 and 300 epochs.

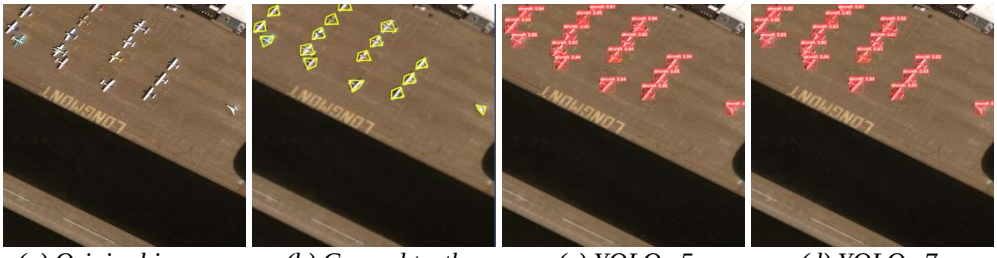

(a) Original image *(b) Ground truth* *(c) YOLO v5* *(d) YOLO v7*

Fig. 5. Visible aircraft detection instance segmentation results of state-of-the-art YOLOv5 and YOLOv7 on the test set of Rareplanes. (a) shows the original image and (b) shows the ground truth. (c) and (d) shows the predicted results.

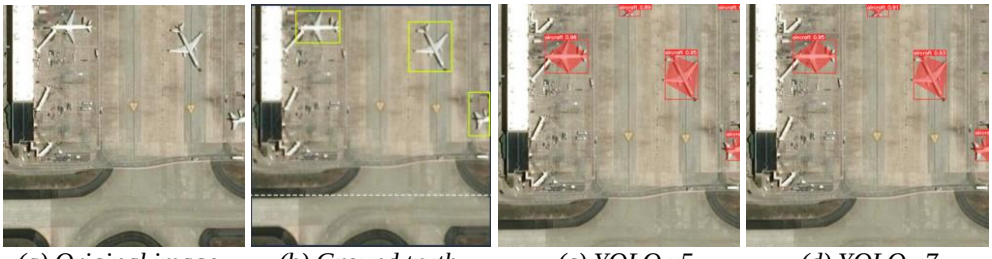

(a) Original image *(b) Ground truth* *(c) YOLO v5* *(d) YOLO v7*

Fig. 6. Visible aircraft detection instance segmentation results of state-of-the-art YOLOv5 and YOLOv7 on the test set of Airbus Aircraft. (a) shows the original image and (b) shows the ground truth. (c) and (d) shows the predicted results.

We have selected the representative scenes in the test set of both Rareplanes and Airbus aircraft detection datasets for instance segmentation. Visualization of the results is shown in Fig. 5. As shown Fig. 5 represents the image of the RarePlanes test set and Fig. 6 represents the Airbus test set. Fig. 5, 6 (a) are the original images, (b) are the ground truth of bounding boxes that appear as green, (c) and (d) shows the instance segmentation results of YOLOv5 and YOLOv7 distinguishing with red bounding boxes with predicted mask in instance segmentation can depict the aircraft which is beneficial to determine small and large aircraft with the area covered by an aircraft.

(a) *(b)* *(c)* *(d)*

Fig. 7. Visible aircraft detection of Yolov5 and Yolov7 state-of-the-art instance segmentation models on complex segmentation scenes from satellite data of Mumbai airport. (a) and (b) comparison of predicted results on 3-Band RGB satellite data. (c) and (d) comparison of predicted results on Panchromatic (PAN) satellite data.

Further, examine the migration of instance segmentation models; we have obtained a panoramic Maxar 8-bit panchromatic and multi-spectral remote sensing imagery over Mumbai, Pune, and Ahmedabad airport with multiple types of aircraft or the experiment. Detailed descriptions as shown in Table 1. Fig. 6 (a) and (b) visualize the comparison of YOLOv5 and YOLOv7 on multi-spectral data of Mumbai airport. Fig.6 (c) and (d) visualize the comparison of YOLOv5 and YOLOv7 on panchromatic data of Mumbai airport. The trained models perform well in detecting the aircraft in multi-spectral imagery. However, YOLOv5 performed a higher number of false detection and missing detection compared to YOLOv7 because of similar features to the aircraft over the airport as shown in Table 4.

Figure	**Model**	**Total Aircrafts**	**Correct Prediction**	**False Prediction**	**No. of Undetected Aircraft**
Fig. 6 (a)	YOLOv5	56 Aircrafts	52	01	04
Fig. 6 (b)	YOLOv7		55	01	01
Fig. 6 (c)	YOLOv5		54	02	02
Fig. 6 (d)	YOLOv7		56	01	00

Table 4. Comparison statistics of YOLOV5 and YOLOv7 over Mumbai airport.

(a) (b) (c) (d)

Fig. 7. (Continued.) Visible aircraft detection of Yolov5 and Yolov7 state-of-the-art instance segmentation models on complex segmentation scenes. (a) and (b) comparison of predicted results on 3-Band RGB satellite data of Ahmedabad airport. (c) and (d) comparison of predicted results on Panchromatic (PAN) satellite data of Pune airport.

Fig. 8 (a) and (b) visualize the comparison of YOLOv5 and YOLOv7 on multi-spectral data of Ahmedabad airport. Fig.7 (c) and (d) visualize the comparison of YOLOv5 and YOLOv7 on panchromatic data of Pune airport. As shown in the above figures YOLOv5 showed a higher number of false detection and missing detection compared to YOLOv7 on panchromatic imagery of airports because panchromatic single band greyscale imagery combines the feature

of aircraft with the other objects that increase the false detection and missing detection as shown in Table 5.

Figures	Model	Total aircrafts	Correct Prediction	False Prediction	No. of Undetected Aircraft
Figure 7 (a)	YOLOv5	10 Aircrafts	06	03	04
Figure 7 (b)	YOLOv7		10	02	00
Figure 7 (c)	YOLOv5	17 Aircrafts	12	01	05
Figure 7 (d)	YOLOv7		15	01	02

Table 5. Comparison statistics of YOLOV5 and YOLOv7 over Ahmedabad and Pune airport.

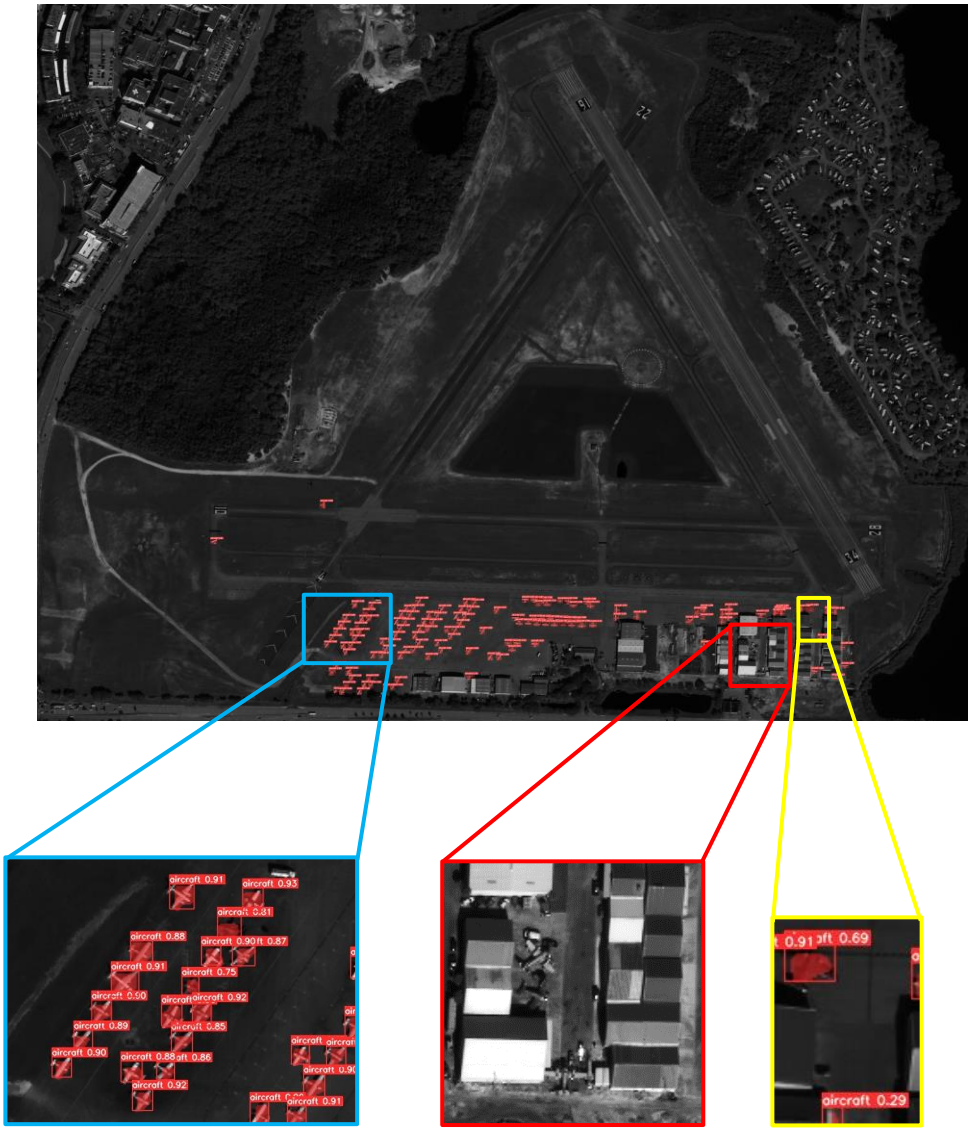

Fig. 9. Aircraft detection result on 16-bit Panchromatic (PAN) Maxar satellite imagery of

YOLOv7. Blue box shows the true detection, red box shows the no detection and yellow box shows the false detection results.

8 Discussion

In this paper, we have utilized the present "state-of-the-art" instance segmentation models and the used very high-resolution remote sensing satellite data to detect and count number of aircrafts. For the Ahmedabad airport, our models correctly detected and counted 96% of aircraft on multi-spectral and 98% on panchromatic satellite data with 1% of false detection. Over Mumbai and Pune data, our models correctly detected and counted the 100% and 88% aircraft with 2% of false detections which is relatively better than other proposed models for the related problems. We have successfully been able to achieve 99.201% mask mean average precision with the 0.014 segmentation loss. After analyzing and evaluating model performances, we conclude that models used in this exercise were not able to further optimize the segmentation loss and improve the mean average precision due to some challenges. Our model is trained on the data over different regions, dimensions, imaging angles and visibility but it was trained on world view-3 and SPOT sensors. Dynamic ranges and spatial resolution of worldview-3 and SPOT sensors is not similar to that of Indian remote sensing sensors. Moreover, we only had very limited amount of data over airports from Indian remote sensing satellites. So, we used the technique of transfer learning to detect aircrafts over Indian remote sensing data. We could achieve accuracy of better than 94% for larger aircrafts detection and above 88% for detection of smaller aircraft over Indian data. Accuracy was relatively lower over detection of smaller aircraft due to insufficient amounts of training dataset for this class. Due to limited period, we were not able to diverse our dataset to the extend and improve the model performance further. We believe that our proposed instance segmentation models have a potential to develop a generic solution to the task of change detection and 3D modelling of aircrafts.

9 Conclusion and Future Scope

In this research, we have implemented the "State-Of-The-Art" instance segmentation models YOLOv5 and YOLOv7 on high-resolution satellite datasets (~25,000 images) of CosmiQ RarePlanes and Airbus Aircraft Detection and trained on 50, 100, and 300 epochs using hyper-parameters to improve the accuracy and performance of models. We have selected metrics parameters like segmentation loss, object loss, bounding box loss, precision (P), recall (R), and mean average precision (mAP) to compare the two models. During training at 50 epochs, YOLOv5 improved the segmentation loss and mean average precision (mAP) by 2% at IoU 0.95 compared to YOLOv7 with an accuracy above 53% to segment smaller aircraft. After continuing to 100 epochs, YOLOv7 mask mAP improved to 0.9903 at 0.5 IoU threshold comparatively YOLOv5 dropped the mAP by 1%. At best 300 epochs, YOLOv7 showed the improvement in training and validation losses with mask mAP of 99.201% under 0.5 IoU comparatively YOLOv5 mask mAP of 99.125% under 0.5 IoU. We implemented the models on panchromatic and multi-spectral remote sensing data of Indian remote sensing satellites over Mumbai, Pune, and Ahmedabad airports and obtained an accuracy of above 94% to segment large aircraft and above 88% to segment smaller aircraft.

In the future, we will extend this study to implement the instance segmentation techniques on C-Band (0.3 – 0.5m Very High Resolution) Synthetic Aperture Radar (SAR) satellite data to make it a universal solution to detect aircraft in any satellite imagery and improve the performance. Further, we are planning to improve the accuracy and implement this solution on satellite data of airports at the national level as well as techniques that will use to perform automatic change detection in multiple scenes.

10 References

[1] A. Singh and M. J. Nene, "Aircraft Detection in Satellite Images," 2022 International Conference on Futuristic Technologies (INCOFT), Belgaum, India, 2022, pp. 1-5, doi: 10.1109/INCOFT55651.2022.10094468.

[2] Shenglong Chen, Yoshiki Ogawa, Chenbo Zhao, Yoshihide Sekimoto, Large-scale individual building extraction from open-source satellite imagery via super-resolution-based instance segmentation approach, ISPRS Journal of Photogrammetry and Remote Sensing, Volume 195, 2023, Pages 129-152, ISSN 0924-2716, https://doi.org/10.1016/j.isprsjprs.2022.11.006.

[3] T. Wang, M. Liu, H. Zhang, X. Jiang, Y. Huang and X. Jiang, "Landslide Detection Based on Improved YOLOv5 and Satellite Images" 2021 4th International Conference on Pattern Recognition and Artificial Intelligence (PRAI),Yibin,China,2021,pp.367-371, doi: 10.1109/PRAI53619.2021.9551067.

[4] S. Wei, X. Zeng, Q. Qu, M. Wang, H. Su and J. Shi, "HRSID: A High-Resolution SAR Images Dataset for Ship Detection and Instance Segmentation," in IEEE Access, vol. 8, pp. 120234-120254, 2020, doi: 10.1109/ACCESS.2020.3005861.

[5] İ. Karakaya, B. Demirel, O. Öztörk, M. Bal and E. Başeski, "HVLSeg: An Ensemble Model for Instance Segmentation on Satellite Images," 2020 28th Signal Processing and Communications Applications Conference (SIU), Gaziantep, Turkey, 2020, pp. 1-4, doi: 10.1109/SIU49456.2020.9302122.

[6] M. Polat, H. M. A. Mohammed, E. A. Oral and I. Y. Ozbek, "Aircraft Detection from Satellite Images Using ATA-Plane Data Set," 2019 27th Signal Processing and Communications Applications Conference (SIU), Sivas, Turkey, 2019, pp. 1-4, doi: 10.1109/SIU.2019.8806582.

[7] L. Mou and X. X. Zhu, "Vehicle Instance Segmentation From Aerial Image and Video Using a Multitask Learning Residual Fully Convolutional Network," in IEEE Transactions on Geoscience and Remote Sensing, vol. 56, no. 11, pp. 6699-6711, Nov. 2018, doi: 10.1109/TGRS.2018.2841808.

[8] H. Wu, H. Zhang, J. Zhang and F. Xu, "Fast aircraft detection in satellite images based on convolutional neural networks," 2015 IEEE International Conference on Image Processing (ICIP), Quebec City, QC, Canada, 2015, pp. 4210-4214, doi: 10.1109/ICIP.2015.7351599.

[9] Z. -Q. Zhao, P. Zheng, S. -T. Xu and X. Wu, "Object Detection with Deep Learning: A Review," in IEEE Transactions on Neural Networks and Learning Systems, vol. 30, no. 11, pp. 3212-3232, Nov. 2019, doi: 10.1109/TNNLS.2018.2876865.

[10] Syed Sahil Abbas Zaidi, Mohammad Samar Ansari, Asra Aslam, Nadia Kanwal, Mamoona Asghar, Brian Lee, A survey of modern deep learning based object detection models, Digital Signal Processing, Volume 126, 2022, 103514, ISSN 1051-2004, https://doi.org/10.1016/j.dsp.2022.103514.

[11] Mohanty, Sharada & Czakon, Jakub & Kaczmarek, Kamil & Pyskir, Andrzej & Tarasiewicz, Piotr & Kunwar, Saket & Rohrbach, Janick & Luo, Dave & Prasad, Manjunath & Fleer, Sascha & Göpfert, Jan & Tandon, Akshat & Mollard, Guillaume & Rayaprolu, Nikhil & Salathe, Marcel & Schilling, Malte. (2020). Deep Learning for Understanding Satellite Imagery: An Experimental Survey. Frontiers in Artificial Intelligence. 3. 10.3389/frai.2020.534696.

[12] Hafiz, A.M. and Bhat, G.M., 2020. A survey on instance segmentation: state of the art. International journal of multimedia information retrieval, 9(3), pp.171-189.

[13] He, K., Gkioxari, G., Dollár, P. and Girshick, R., 2017. Mask r-cnn. In Proceedings of the IEEE international conference on computer vision (pp. 2961-2969).

[14] Chen, H., Sun, K., Tian, Z., Shen, C., Huang, Y. and Yan, Y., 2020. Blendmask: Top-down meets bottom-up for instance segmentation. In Proceedings of the IEEE/CVF conference on computer vision and pattern recognition (pp. 8573-8581).

[15] Redmon, Joseph, Santosh Kumar Divvala, Ross B. Girshick and Ali Farhadi. "You Only Look Once: Unified, Real-Time Object Detection." 2016 IEEE Conference on Computer Vision and Pattern Recognition (CVPR) (2015): 779-788.

[16] Peiyuan Jiang, Daji Ergu, Fangyao Liu, Ying Cai, Bo Ma, A Review of Yolo Algorithm Developments, Procedia Computer Science, Volume 199, 2022, Pages 1066-1073, ISSN 1877-0509, doi.org/10.1016/j.procs.2022.01.135.

[17] Shermeyer, J., Hossler, T., Van Etten, A., Hogan, D., Lewis, R., and Kim, D., "RarePlanes: Synthetic Data Takes Flight", arXiv e-prints, 2020. doi:10.48550/arXiv.2006.02963.

[18] Airbus Aircraft Detection Sample Dataset of satellite imagery on kaggle, https://www.kaggle.com/datasets/airbusgeo/airbus-aircrafts-sample-dataset

[19] He, K., Zhang, X., Ren, S., & Sun, J. (2014). Spatial Pyramid Pooling in Deep Convolutional Networks for Visual Recognition. IEEE Transactions on Pattern Analysis and Machine Intelligence, 37, 1904-1916.

[20] Liu, S., Qi, L., Qin, H., Shi, J., & Jia, J. (2018). Path Aggregation Network for Instance Segmentation. 2018 IEEE/CVF Conference on Computer Vision and Pattern Recognition, 8759-8768.

[21] Ultralytics YOLO v5 "State-Of-The-Art" Instance segmentation model official repository, https://github.com/ultralytics/yolov5

[22] Zhu, Wenbo, Quan Wang, Lufeng Luo, Yunzhi Zhang, Qinghua Lu, Wei-Chang Yeh, and Jiancheng Liang. 2022. "CPAM: Cross Patch Attention Module for Complex Texture Tile Block Defect Detection" Applied Sciences 12, no. 23: 11959. https://doi.org/10.3390/app122311959

[23] Wang, C.Y., Bochkovskiy, A., and Liao, H.-Y. M., "YOLOv7: Trainable bag-of-freebies sets new state-of-the-art for real-time object detectors", arXiv e-prints, 2022. doi:10.48550/arXiv.2207.02696